IOP Conference Series: Materials Science and Engineering

PAPER • OPEN ACCESS

Study hydrogen embrittlement and determination of E110 fuel cladding mechanical properties by ring compression testing

To cite this article: H K Namburi *et al* 2018 *IOP Conf. Ser.: Mater. Sci. Eng.* **461** 012059

Study hydrogen embrittlement and determination of E110 fuel cladding mechanical properties by ring compression testing

H K Namburi [1], L Ottazzi [1, 2], M Chocholousek [1], G Lomonaco [2], P Gavelova [1], J Krejci [3]

[1] Centrum výzkumu Řež s. r. o., Husinec-Řež, 252 63 Czech Republic

[2] GeNERG-DIME/TEC, University of Genova, via all'opera Pia 15/A, 16145 Genova, Italy

[3] UJP PRAHA a.s., Praha – Zbraslav, Czech Republice, EU

E-mail: nab@cvrez.cz

Abstract. Zirconium based alloys are commonly used as material for fuel claddings in the light water reactors. Claddings act as first metallic barriers against loss of fission products during the nuclear power plant operation, intermittent storage or final dry storage. The integrity of claddings is always critical issue during reactor operation and during storage of spent fuel. In this work, ring compression testing method developed was applied to study hydrogen embrittlement, to evaluate the stress–strain behaviour and hoop fracture properties of E110 (Zr-based) fuel claddings. The results show that the collapse load and the tensile strength values depend strongly on hydrogen concentration. In particular, tensile strength experiment data shows significant change in its trend after reaching the maximum hydrogen solubility limit.

1 Introduction

Zirconium based fuel claddings serve as barrier between the pellets and the fuel rod environment, avoiding the release of fuel or fission products during service into the reactor core or cooling system or after service into storage containments. Zirconium and its alloys have a significant property, a very low neutron absorption cross section, 30 times less than iron. In addition, zirconium alloys also possess good corrosion resistance, mechanical strength and are relatively resistant to radiation damage [1-3]. During the reactor operation, claddings accumulate hydrogen due to oxidation and are subjected to degradation resulting from their exposure to high temperature, high pressure and irradiation. When the hydrogen content in zirconium alloys exceeds the terminal solid solubility limit, diffused hydrogen atoms react with the zirconium matrix and formation of zirconium hydrides occurs [3]. The amount of hydrogen increases with the increase in the fuel burn-up and reactor operation time reactor cycles [4]. Possible degradation mechanisms of fuel claddings include creep, hydrogen embrittlement (reduction in ductility) are reported in detail in and delayed hydride cracking [5-12] etc. Under the influence of internal pressure, temperature, hydrogen content claddings may undergo failure. Therefore the study on mechanical integrity of the fuel cladding tubes is very important.

When the hydrogen solubility limit in zirconium based alloys exceeds, the excess amount of it results in the formation of zirconium hydride as precipitates. These precipitates have been shown to be less ductile than the surrounding zirconium alloy matrix, so can have deleterious effects on the mechanical properties. It has been demonstrated that these hydrides may embrittle the cladding and reduces its mechanical strength. The resulting embrittlement depends on the concentration and geometrical distribution of the hydrides [16-20]. Current study is focused on evaluating the mechanical properties in the hoop direction of the zirconium based fuel cladding (E110) with different hydrogen contents (as received, 120, 283, 1500 wt. ppm) using the Ring Compression Testing technique at RT-150-400 °C. And furthermore, to determine the best practices for testing irradiated claddings in hot-cells to perform cladding embrittlement studies.

2 Materials and Methods

2.1. Materials and Methods

Specimen examined in this study was fabricated from E110 alloy of tubular section, 10 mm long with outer diameter of ~ 9.1 mm and wall thickness of ~ 570 µm provided by UJP Prague. The chemical composition of E110 cladding tube was 99 % Zr and 1 % Nb with minor impurities of Fe and O. Metallography was performed before mechanical testing, to determine hydrides distribution in pre-hydrogenated specimens. Ring compression testing is performed in the present study in order to obtain the mechanical properties of tubular samples in hoop direction with various hydrogen content at different hydrogen content as in Table 1 using Zwick Z250 test machine. The thermo-mechanical cycle is shown in Figure 1 and Zwick machine with flat compression holders are shown in Figure 2. Test was performed in displacement control mode at 0.5 mm/min.

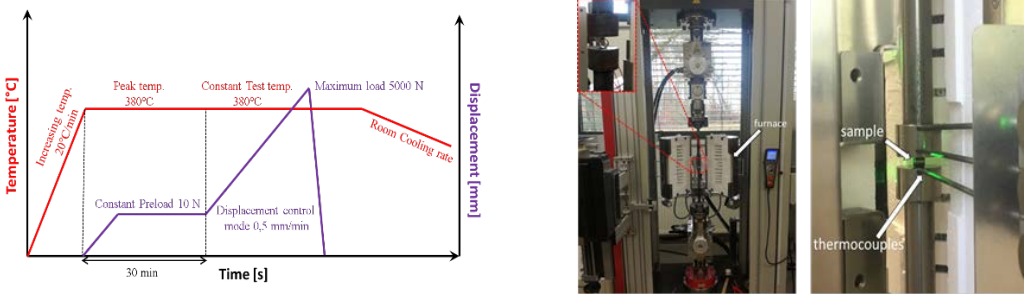

Figure 1. Thermo-mechanical cycle during RCT & **Figure 2**. Ring compression testing machine : (a) Furnace and compression heads; (b) Thermocouples inserted into furnace close to specimen during the RCT

Table 1. Specimen test matrix for ring compression testing to study hydrogen embrittlement in E110 fuel claddings

Hydrogen content (ppm)	Test Temperatures (°C)	Lengths (mm)
As -received	RT-150-400 °C	9.90 - 10.40
120	RT-150-400 °C	9.90 – 10.50
283	RT-150-400 °C	9.90 – 10.30
1500	RT-150-400 °C	9.90 – 10.20

3 Results and Discussion

3.1. Microstructural investigations

Transverse (cross-sectional) and longitudinal metallographic images from the pre-hydrogenated specimens are shown in Figure 3. Optical examination of the hydrogenated metallographic specimens revealed the presence of hydride platelets aligned in circumferential direction. These are called circumferential hydrides formed on the circumferential-longitudinal planes and were in the form of long chains. The average length of macro-hydrides in the circumferential and longitudinal direction was about 150 -182 µm. Figure 4 shows the 3D re-construction of the observed hydrides on the

circumferential-longitudinal plane. On the right side of this figure, the habit planes of the circumferential hydrides in hexagonal zirconium lattice are shown.

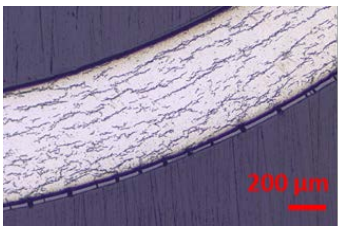

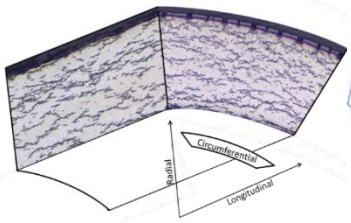

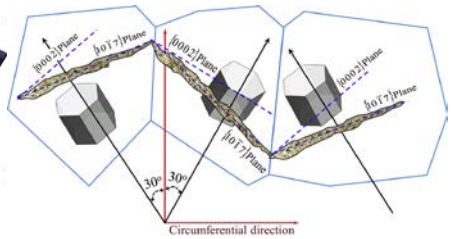

Figure 3. Hydrides oriented in the radial-circumferential orthographic plane & **Figure 4.** (a) 3D reconstruction of hydrides orientation in the creep tested hydrided E110 cladding; (b) schematic of hydride formation on habit plane [21]

3.2. Mechanical investigations

Load – displacement curves obtained from ring compression testing at various levels of hydrogen content tested at RT-150-400 °C are shown in Figure 5. On the recorded load-time curve, three areas was highlight to show the macroscopic behavior of the sample during RCT. Figure 6 represents the deformation stages of cladding during the ring compression test with varying loading at constant temperature. Initially there was a linear relationship between the stress and the strain. The next stage, known as plastic deformation zone, where drastic change of slope is noticeable. During RCT, it is known that sample underwent plastic deformation after initial elastic deformation. As shown in Figure 7, the collapse force P_0, where large plastic deformation occurred, can be obtained directly from the load-displacement curve by getting the intersection of the lines extended from elastic and plastic region, respectively. After extracting collapse force from the load-displacement curve, one of targeted properties of the material, ultimate tensile stress (UTS), could be estimated by the equations provided from previous works [22-23], which were based on theoretical models of plastic theory and several basic mechanical theories. Thus, the dimensions of sample as in Figure 7(b), including outer radius *R*, thickness *t* and length *L*, are important factors in these equations which aim to convert collapse force into UTS. Due to the complexity of the stress distribution in the sample, the ring is assumed to be perfectly plastic, which means no working hardening occurred in the whole process of RCT. With the plastic theory, the correlation between collapse stress σ_0 and plastic moment M_p can be obtained by

$$M_p = 1/4\ \sigma_0\ t^2\ L \quad (1)$$

Where, M_p is defined as the moment, at which the entire cross section is under its yield stress. Furthermore, based on the law of conservation of energy, the external virtual work done by P_0 is known to be equal the internal virtual work done by M_p. Thus, the collapse force can be defined as

$$P_0 = (4\ M_p) / R = (\sigma_0\ t^2\ L) / R \quad (2)$$

For working hardening material, a similar correlation can also be established and be used to get the collapse stress σ_0, as shown below:

$$\sigma_0 = \alpha\ P_0\ R / (t^2\ L) \quad (3)$$

Note that the constant α equals 0.866 in this work because the value of α depends upon the lengths of sample. Collapse stress is calculated from RCT, and then can be linearly correlated to the UTS of tensile test through the following coefficients

$$R_m = \sigma_0 / K_{UTS} \quad (4)$$

The load-displacement curves obtained from the RCT are shown in Figure 5, basically demonstrates two different types of results. It is evident from that the samples with lower wt. ppm H without hydrides have the point of contact between the upper and lower face (where there is the huge change of slope) higher than the other concentrations. This indicates that the samples with a higher hydrogen concentration were less ductile, due to the precipitation of δ-hydrides in the sample. The tests carried out at room temperature exhibits large cracks at the equatorial azimuths. These cracks initiate at the outer surface of the ring and propagate toward the inner surface. The crack depth in the sample with 120 and 283 wt. ppm is about half of the cladding thickness and the whole thickness in the samples with more than 1500 ppm. It may be observed that higher the

hydrogen content, the smaller the number of steps in the main crack. This is consistent with easier propagation in the axial direction of the samples. Furthermore, low H content, ductile fracture occurs by formation and growth of voids. For the specimens with high H content brittle areas appeared, indicating fracture through hydrides.

The tests developed from room temperature to the set temperature of 150 °C, showed a different tensile strength compared to the tests a room temperature. In this case cracks were never observed until 1500 ppm, where the high amount of hydrides caused the loss of ductility and the formation of crack in the load-displacement curve close to 7 mm and 8 mm. The samples with 120 and 283 wt. ppm recovered their ductility as temperature increased. In these results, we can suppose two possibilities: precipitated zirconium hydrides may become ductile at 150 °C or a Zr metal matrix may regain enough ductility to accommodate the large plastic deformation even with the brittle hydride precipitates (the solubility of the zirconium matrix at this temperature is about 10 ppm). However, many studies at 150 °C suggest that the hydrides are still brittle at that temperature but the ductility of matrix improves with the increase of temperature. In addition, specimens regain their ductility at relatively high temperature above 250 °C, regardless of hydride orientation, supports the matrix recovery theory. As would expected, the load-displacement curves at 400 °C show that all the specimens can deform substantially without cracking. This implies that the Zr-matrix recovers its ductility enough to bear a large plastic deformation at 400 °C. This indicates that at this high temperature, common in the dry storage, these hydrides cannot act as a crack initiation site. At this temperature the hydrogen solubility is about 210 wt. ppm that means the specimen with 120 wt. ppm did not present hydrides, so the whole amount of hydrogen presented in the specimen was dissolved in the α-Zr. The tensile strengths R_m, which could be obtained by converting the collapse loads with Equations. (3) - (4) are summarized in Table 2.

Figure 8, shows the tensile strength behavior of E110 fuel claddings tested with various hydrogen contents at different test temperatures. The experimental results showed that this test is very sensitive to low hydrogen concentration, for 120 wt. ppm of hydrogen produce a noteworthy effect in the load vs. displacement curves. The analysis was performed to identify the fracture behavior and compare the as-received with the pre-hydrided samples at the main temperature that the cladding undergoes during its whole life. In all cases the tests showed that the increase of hydrogen leads to a decrease of fracture strain or loss of ductility. Moreover, at 400 °C and high hydrogen concentrations the E110 exhibits an almost ideal elastic-plastic behavior. A remarkable increase of the ultimate tensile strength is observed for the samples with 120 wt. ppm, whereas for the concentrations in excess of 120 wt. ppm, the UTS increases slowly.In the tests with the presence of circumferential δ-zirconium hydrides into the samples parallel to applied stress causes an increase of tensile strength due to the presence of harder (always more brittle) particles within the microstructure. The hydrides absorb more load than Zr-matrix causing the increase of the tensile strength. On the other hand the tests developed with 189 wt. ppm demonstrated the no presence of hydrides owing to the solubility (about 216 wt. ppm) at 380 °C. That means that the hydrogen was all in solid solution.

Table 2. Tensile strength (R_m) at RT-150-400 °C with different hydrogen content

Hydrogen content (ppm)	Average R_m at RT (MPa)	Average R_m at 150 °C (MPa)	Average R_m at 400 °C MPa)
0	379.31	264.98	166.52
120	434.99	310.84	192.76
283	444.35	321.26	192.19
1500	492.35	323.60	237.12

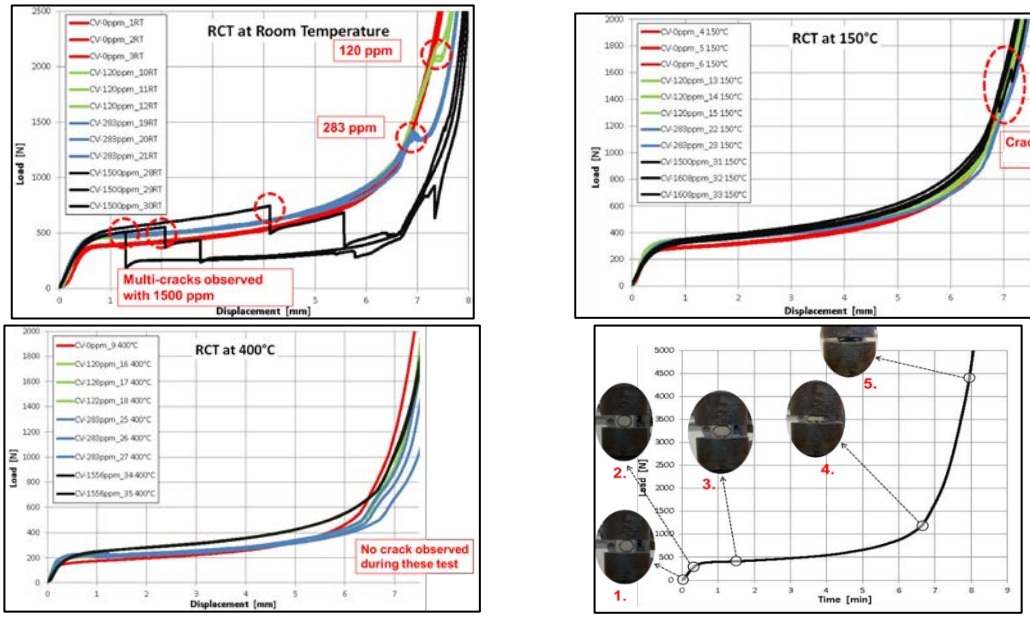

Figure 5. Load-displacement curves from RCT tests with different hydrogen concentration at RT-150-400 °C and **Figure 6.** Stages of cladding tube deformation during the ring compression testing at room temperature

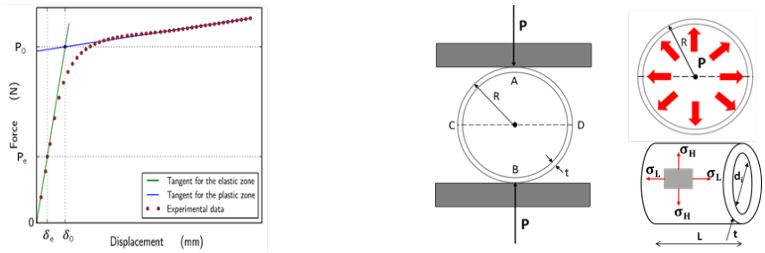

Figure 7. (a) Load-displacement curve of ring compression test; (b) Schematic of test specimen during ring compression testing

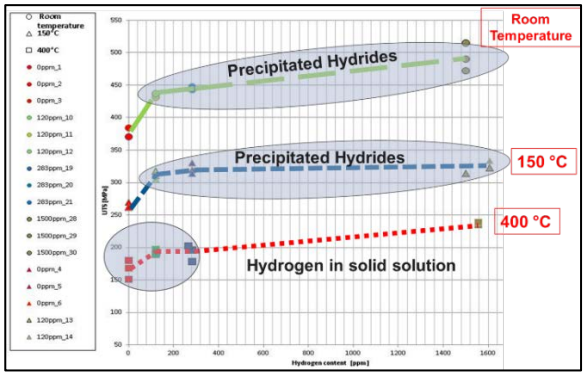

Figure 8. Tensile strength at RT-150-400 °C with different hydrogen concentrations

4. Conclusions

The experimental results showed that RCT test is very sensitive to low hydrogen concentration in test sample. The presence of δ-hydrides in the matrix causes an increase of tensile strength due to its harder properties. RCT test is an interesting test method to determine mechanical properties in hoop direction of tubular samples. Its cost-reducing and the low material consumption gave the test a real potential.

References

[1] C. Lemaignan.; Arthur T. Motta. Zirconium Alloys in Nuclear Applications. Materials Science and Technology: A Comprehensive Treatment 1994, vol. 10, pp. 1-51.
[2] Konings. Rudy. Zirconium Alloys: Properties and Characteristics. Comprehensive Nuclear Materials 2012, vol. 2, pp. 217–232.
[3] H. Okamoto. H-Zr (Hydrogen-Zirconium). Journal of Phase Equilibria and Diffusion 2006, no. 27, pp. 548-549.
[4] D. Kook Review of spent fuel integrity evaluation for dry storage. Nuclear Engineering and Technology 2013, vol. 45, pp. 115-124.
[5] T. Alam. A review on the clad failure studies. Nuclear Engineering and Design 2011, pp. 3658–3677.
[6] S. Suman. Hydrogen in Zircaloy: Mechanism and its impacts. International Journal of Hydrogen Energy 2015, pp. 5976–5994.
[7] F. Feria. ; L.E. Herranz . Creep assessment of Zry-4 cladded high burnup fuel under dry storage. Progress in Nuclear Energy 2011, pp. 395-400.
[8] R.N. Singh. Stress-reorientation of hydrides and hydride embrittlement of Zr–2.5 wt% Nb pressure tube alloy. Journal of Nuclear Materials 2004, no. 325, pp. 26–33.
[9] Hygreeva K. Namburi.; K. S. Valance.; J. Bertsch. Delayed hydride cracking in Zircaloy-2 fuel cladding tubes. TopFuel Reactor Fuel Performance 2012.
[10] Y. S. Kim. Precipitation of reoriented hydrides and texture change of α-zirconium grains during delayed hydride cracking of Zr-2.5Nb pressure tube. Journal of Nuclear Materials 2001, no. 297, pp. 292-302.
[11] R. N. Singh. Influence of temperature on threshold stress for reorientation of hydrides and residual stress variation across thickness of Zr–2.5Nb alloy pressure tube. Journal of Nuclear Materials 2006, no. 359, pp. 208–219.
[12] K. Kese Hydride re-orientation in Zircaloy and its effect on the tensile properties. SKI report 98:32 1998, pp. 49.
[13] Hyun-Gil Kim. The effects of creep and hydride on spent fuel integrity during interim dry storage. Nuclear Engineering and Technology 2010, vol. 42, no. 3, pp. 249-258.
[14] K.Kese Threat of hydride re-orientation to spent fuel integrity during transportation accidents: Myth or reality? In Proceedings of the 2007 International LWR Fuel Performance Meeting, San Francisco, 2007. pp.464-471.
[15] Hyun-Jin Cha. The effect of hydrogen and oxygen contents on hydride reorientations of zirconium alloy cladding tubes. Nuclear Engineering Technology 2015, no. 147, pp. 746-755.
[16] S.Arsene.; J. B. Bai. Effet de la microstructure et de la temperature sur la transition ductile-fragile des Zircaloy hydrurés, PhD dissertation, Ecole Centrale Paris, 1997.
[17] J. Desquines.; B. Cazalis.; Bernernaudat.; Ch.Poussard.; X. Averty.; P.J. Yvon. ASTM Int. 2 (6), 2005, Paper ID JAI 12465.
[18] G.W. Parry .; W.Evans. Nucleonics. 1964, no. 22, pp. 65.
[19] A.C.Wallace.; G.K Shek.; O.E. Lepik. ASTM Spec. Tech. Publ 1989, no. 1023, pp. 66–88.
[20] K.Linga.; I.Charit. Texture development and anisotropic deformation of Zircaloys. Progress in Nuclear Energy 2006, no. 48, pp. 325-359.
[21] S. Suman. Hydrogen in Zircaloy: Mechanism and its impacts. International Journal of Hydrogen Energy 2015, no. 40, pp. 5976 – 5994.
[22] V.Busser.; M.C.Baietto-Dubourg.; J.Desquines.; C.Duriez.; J.P.Mardon. Mechanical response of oxidized Zircaloy-4 cladding material submitted to a ring compression test. Journal of Nuclear Material 2009, no. 384, pp. 87-95.
[23] Y.T.Reddy.; S.R.Reid. On obtaining material properties from the ring compression test. Nuclear Engineering and Design, 1979, no. 52, pp. 257-263.